DOI: 10.1002/ejic.200701134

Comparing Models for $S = 1/2$ Heisenberg Antiferromagnetic Chains: The Validity of Different Approaches for Describing a One-Dimensional Coordination Polymer, $[Cu^{II}(HL)_2(4,4'\text{-bpy})]_n \cdot 2nH_2O$ (H_2L = 3-Nitrophthalic Acid, bpy = Bipyridine)

Yu-Heng Deng,*[a] Juan Liu,[a] Biao Wu,[b] Christina Ambrus,[c] Tony D. Keene,[c] Oliver Waldmann,*[c][‡] Shi-Xia Liu,*[c] Silvio Decurtins,[c] and Xiao-Juan Yang[b]

Keywords: Magnetism / Low-temperature studies / Copper / Bridging ligand / Crystal structure

We have synthesized a new one-dimensional coordination polymer, $[Cu^{II}(HL)_2(4,4'\text{-bpy})]_n \cdot 2nH_2O$ (**1**), (HL^- = monodeprotonated 3-nitrophthalic acid, 4,4′-bpy = 4,4′-bipyridine) consisting of infinite chains of $[Cu^{II}(HL)_2(4,4'\text{-bpy})]_n$ and have investigated its structure and magnetic properties. Compound **1** crystallizes in the monoclinic $C2/c$ space group with the $[Cu^{II}(HL)_2(4,4'\text{-bpy})]_n$ chains running parallel to the b axis. The chains are linked together by hydrogen bonding between the HL^- groups and water molecules to form the three-dimensional crystal structure. The magnetic susceptibility of **1** can be well described using an antiferromagnetic $S = 1/2$ chain model with $g = 2.11(1)$ and $2J = -0.61(1)$ cm^{-1}. Several techniques for describing the susceptibility of $S = 1/2$ chains are examined to compare their validity at low values of $kT/|2J|$, including exact numerical full-matrix diagonalization techniques, from which the magnetization curve of **1** could be calculated. The calculation fits well with the measured magnetization data.

Introduction

The 4,4′-bipyridine ligand has proven to be a very versatile building block for the synthesis of coordination compounds of transition metal ions with different network architectures. Examples include 1D chains formed by cobalt, manganese, nickel, and copper ions as paramagnetic centres,[1–3] 2D grids or sheets,[1,4–5] and 3D networks constructed of $[Cu^{II}(4,4'\text{-bpy})]^{2+}$ units.[6–8] The arenedicarboxylic acids – for example, phthalic, isophthalic, and terephthalic acids – are also frequently used in the construction of supramolecular compounds.[9] However, systems combining the two kinds of ligands are only occasionally seen, and only a few structures have been reported so far.[10–12] A close analogue of the bicarboxylic acids is 3-nitrophthalic acid (H_2L), but its complexes are rare. To the best of our knowledge, there is only one Cu^{II} complex with H_2L reported in the literature.[13] We have hence recently started to explore coordination polymers based on H_2L and have obtained a series of transition metal and rare earth complexes.[14,15]

In the present work, we report the synthesis, crystal structure, and in particular, magnetic properties of $[Cu^{II}(HL)_2(4,4'\text{-bpy})]_n \cdot 2nH_2O$ (**1**), which represents the first linear chain of Cu^{II} complexed with the anion of a bicarboxylic acid and 4,4′-bpy. The 1D antiferromagnetic $S = 1/2$ chain model has been heavily investigated in the past because of its role as a key model in quantum magnetism, and numerous approximations to evaluate its magnetic susceptibility, χ, have been developed. Thanks to recent developments in physics, $\chi(T)$ is now fully understood over the whole temperature range, and highly accurate formulas have become available for approximating its behaviour. We have hence examined the various techniques available in the literature for describing the $\chi(T)$ value of $S = 1/2$ 1D chains, and have compared their validity at low values of $kT/|2J|$. The exchange coupling mediated by 4,4′-bpy as a bridging unit in Cu^{II} complexes has been previously studied to some extent, and it was generally found to be very small.[1,10b] In order to confirm the exchange constant derived from $\chi(T)$ and our magnetic modelling of **1**, we also studied the magnetization curve at 1.9 K, which we could simulate using exact numerical full-matrix diagonalization techniques.

[a] Department of Chemistry, Capital Normal University, Beijing 100037, China
E-mail: dyh@mail.cnu.edu.cn
[b] State Key Laboratory for Oxo Synthesis & Selective Oxidation, Lanzhou Institute of Chemical Physics, Chinese Academy of Sciences, Lanzhou 730000, China
[c] Department of Chemistry and Biochemistry, University of Berne, Freiestrasse 3, 3012 Berne, Switzerland
E-mail: liu@iac.unibe.ch
[‡] Present address: Physikalisches Institut, Universität Freiburg, 79104 Freiburg, Germany
E-mail: oliver.waldmann@physik.uni-freiburg.de
Supporting information for this article is available on the WWW under http://www.eurjic.org or from the author.

Results and Discussion

Crystal Structure

Compound **1** is a one-dimensional coordination polymer and crystallizes in the *C*2/*c* space group (Table 1). The asymmetric unit consists of one copper atom, one monodeprotonated 3-nitrophathalic acid (HL^-) ligand, one half of a 4,4′-bpy molecule and one water molecule. As shown in Figure 1, each Cu^{II} ion is coordinated by the deprotonated COO^- groups of two 3-nitrophthalic acid ligands and two 4,4′-bpy molecules to form a *trans*-$N_2O_2+O_2$ set where the N_2O_2 set is in an approximately square plane with Cu(1)–O(1), Cu(1)–N(2), and Cu(1)–N(3) distances of 1.967(2), 2.018(2), and 2.015(2) Å, respectively. Cu(1) and the N(2), C(11), C(12), and N(3) atoms of the 4,4′-bpy molecule lie on a twofold rotation axis (Wyckoff letter e) through which the repeating unit of the coordination polymer, $[Cu(HL)_2(4,4'\text{-bpy})]$, is generated. The 4,4′-bpy molecule bridges two Cu^{II} ions with a Cu···Cu separation of 11.125(1) Å, which leads to the formation of infinite linear $[Cu(4,4'\text{-bpy})]_n^{2n+}$ chains running parallel to the *b* axis (Figure 2). The 4,4′-bpy molecules have a torsion angle of 28.1(2)° between the pyridine groups, while the N–Cu–N angle is 180.0° (C_2 axis). The Cu–O and Cu–N bond lengths and the O–Cu–O bite angles in **1** (Table 2) are similar to those found in the zigzag chains of Cu^{II}–carboxylic acid–4,4′-bpy systems such as, for example, $[Cu(Hsal)_2(4,4'\text{-bpy})]_n$.[10a] The water molecules are involved in hydrogen bonds with the deprotonated [O(1w)···O(1)] and protonated [O(4)···O(1w)] carboxyl groups of 3-nitrophthalic acid from two adjacent chains (Table 3), which extends the 1D chains to a hydrogen-bonded 2D sheet structure in the *ab* plane (Figure 3).

Table 1. Crystallographic data and structure refinement for **1**.

	1
Formula	$C_{26}H_{20}CuN_4O_{14}$
Formula mass	676.00
Crystal system	monoclinic
Space group	*C*2/*c*
a / Å	10.6165(3)
b / Å	11.1249(3)
c / Å	22.9818(5)
β / °	93.712(2)
V / Å^3	2708.63(12)
Z	4
$D_{calcd.}$ / g cm^{-3}	1.658
μ(Mo-K_α) / mm^{-1}	0.890
θ range / °	1.78–28.29
Obsd. data, $I>2\sigma(I)$	2313
R_1 (obsd. data)	0.0392
wR_2 (all data)	0.0952

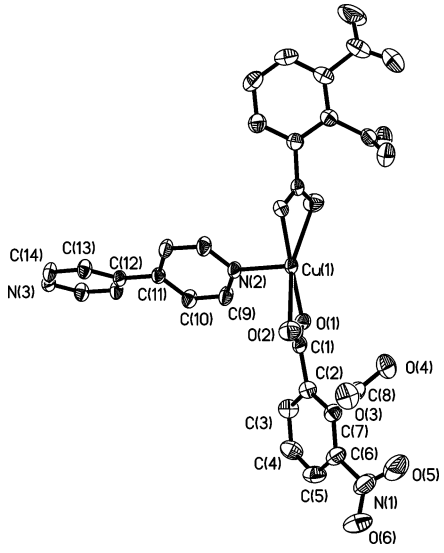

Figure 1. An ORTEP (50% probability ellipsoids) structure of the asymmetric unit and selected symmetry equivalents of **1**. Hydrogen atoms and solvent molecules are omitted for clarity.

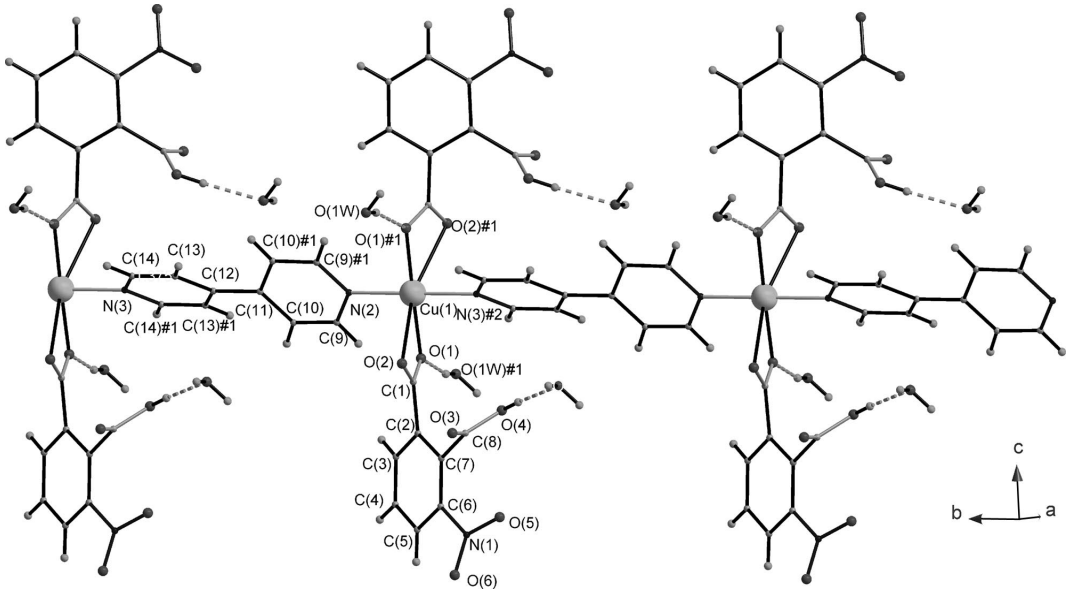

Figure 2. The 1D linear chain of compound **1**.

There are also some short C–H···O contacts between the 4,4′-bpy and the 3-nitrophthalic acid within the chain and two other short contacts with 3-nitrophthalic acid groups in neighbouring chains. The shortest interchain Cu···Cu separation is 7.689(1) Å.

Table 2. Selected bond lengths [Å] and bond angles [°] for **1**.

Bond lengths			
Cu(1)–O(1)	1.967(2)	Cu(1)–O(2)	2.597(2)
Cu(1)–N(2)	2.018(2)	Cu(1)–N(3)[a]	2.015(2)
Bond angles			
O(1)–Cu(1)–O(1)[b]	178.58(8)	O(1)–Cu(1)–O(2)[b]	123.89(6)
N(2)–Cu(1)–N(3)[a]	180.0	O(1)–Cu(1)–O(2)	55.86(6)
N(2)–Cu(1)–O(1)	90.71(4)	N(2)–Cu(1)–O(2)	98.29(4)
O(1)–Cu(1)–N(3)[a]	89.29(4)	N(3)[a]–Cu(1)–O(2)	81.71(4)

[a] Symmetry code: x, $y-1$, z. [b] $-x+1$, y, $-z+1/2$.

Table 3. Selected hydrogen bond lengths [Å] and angles [°] for compound **1**.

D–H···A	*d*(D–H)	*d*(H···A)	*d*(D···A)	∠(D–H···A)
O(4)–H(4)···O(1W)[a]	0.82	1.82	2.634(3)	174.2
O(1W)–H(1WB)···O(1)[b]	0.842	1.927	2.753(3)	166

[a] Symmetry code: $-x+1/2$, $y-1/2$, $-z+1/2$. [b] $1-x$, y, $-z+1/2$.

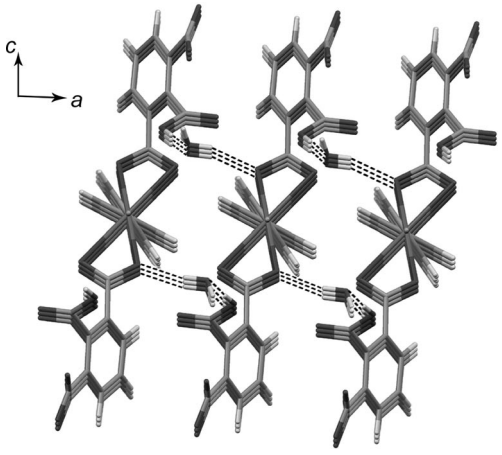

Figure 3. Packing diagram of **1** viewed down the *b* axis and showing the interchain hydrogen bonds between H_2O and $COOH/COO^-$ that lead to a 2D network in the *ab* plane.

Magnetic Properties

The temperature dependence of the $\chi_M T$ product of compound **1** is plotted in Figure 4 (χ_M is the molar susceptibility). The room temperature value of $\chi_M T$ is 0.415 emu K mol^{-1}, which is quite close to the expected value for noninteracting Cu^{II} ions. Upon cooling, $\chi_M T$ remains nearly constant down to about 50 K, below which it starts to drop rapidly. This behaviour is characteristic of compounds with antiferromagnetic exchange interactions between paramagnetic centres, with these being Cu^{II} ions in this case. The interaction, however, must be rather weak, as is evident from the inset to Figure 4, which presents $\chi_M(T)$. The maximum in $\chi_M(T)$ that is expected for an antiferromagnetic system is not observed; that is, it is below the lowest experimentally accessible temperature of 1.9 K. Figure 5 presents the magnetization curve at 1.9 K. At high fields the magnetization starts to saturate, and approaches a value of about 1 $N_A\mu_B$. The field dependence is somewhat similar to that expected for noninteracting Cu^{II} ions, as a comparison with the Brillouin function for $S = 1/2$ ($g = 2.11$) demonstrates. The experimental data, however, lies below the Brillouin curve, which is further evidence for weak antiferromagnetic interactions in the system.

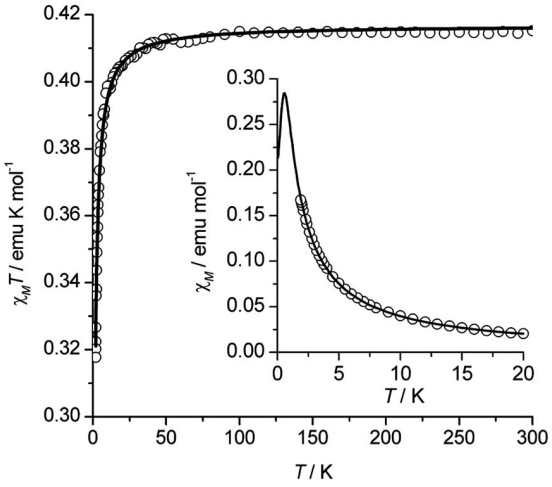

Figure 4. χT (main plot) and magnetic susceptibility (inset) vs. temperature of **1** (open circles). The best-fit curves (solid lines) are based on the formula of Johnston et al. ($2J = -0.61$ cm^{-1}, $g = 2.11$).

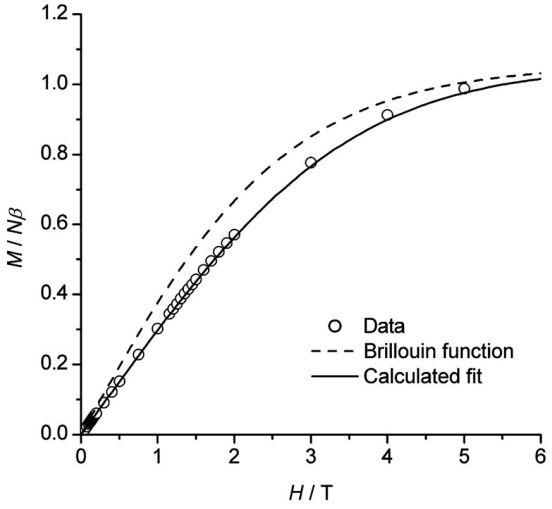

Figure 5. Magnetization vs. field at 1.9 K for **1** (open circles). The dashed curve corresponds to the Brillouin function for a noninteracting Cu^{II} ion (with $g = 2.11$), and the solid line to a finite-size calculation with the parameters $2J = -0.61$ cm^{-1} and $g = 2.11$.

In view of the crystal structure of **1**, the magnetic properties were modelled by a one-dimensional (1D) chain of S = 1/2 sites with isotropic nearest-neighbor Heisenberg exchange interactions, as described by the spin Hamiltonian [Equation (1)]

$$\hat{H}_{1D} = -2J\left(\sum_{i=1}^{n-1}\hat{S}_i \cdot \hat{S}_{i+1} + \hat{S}_n \cdot \hat{S}_1\right) \quad (1)$$

where n denotes the number of Cu^{II} ions in the chain (which approaches infinity in the real compound). Thanks to the remarkable advances in the analytical analyses and numerical algorithms that deal with the magnetic susceptibility of the 1D antiferromagnetic Heisenberg chain ($2J < 0$) in the last 15 years or so, this is now known for all temperatures.[16] This enabled Johnston et al.[17] to develop an approximating function that reproduces the magnetic susceptibility over the whole temperature range with an accuracy better than 10^{-7}, which therefore for any practical purposes can be considered exact (see Supporting Information for the equation). The temperature dependence of the magnetic susceptibility is shown in Figure 6 for g = 2.0 (in this plot the magnetic susceptibility and temperature are given in reduced units; in order to convert to "real" units, the x axis should be multiplied by $|2J|$, and the y axis divided by $|2J|$; to correct for the g factor, the y axis should be multiplied by $g^2/4$). Interestingly, the formula of Johnston et al. also reproduces the logarithmic corrections to the magnetic susceptibility at very low temperatures[16] [at T = 0, the exact value of the magnetic susceptibility is $(1/\pi^2)$-$N_A g^2 \mu_B{}^2 |2J|^{-1}$, or 0.1520 in the units of Figure 6].[16–18]

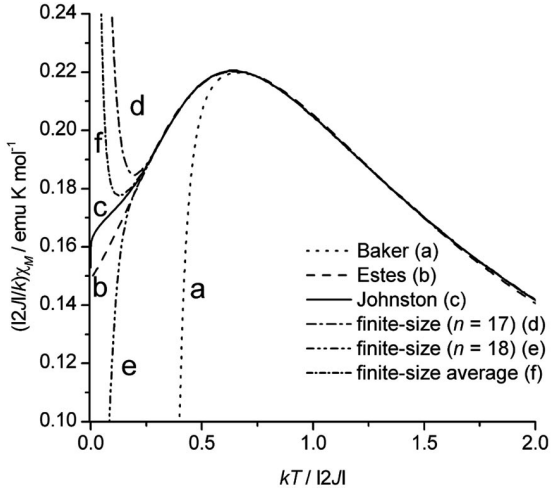

Figure 6. Magnetic susceptibility vs. temperature of a 1D antiferromagnetic S = 1/2 Heisenberg chain as obtained from various available analytical formulas and finite-size calculations (g = 2.0).

In previous work on 1D antiferromagnetic chains, the analysis of the magnetic susceptibility was often based on the analytical formulas proposed by Baker et al.[19] and Estes et al.[20] (see also ref.[21]). Another frequently used technique is finite-size calculations, which are based on the exact numerical diagonalization of the chain model from Equation (1) with a finite number, n, of metal centers.[22] The finite-size calculations will be of special interest to us, since they also permit the calculation of the low-temperature magnetization curve and hence its analysis (vide infra). Using both spin-rotational and spin-permutational symmetry,[23–25] an S = 1/2 chain with n = 18 sites is readily diagonalized on a modern PC (dimension of the Hilbert space = 262,144). The approximation can be improved by taking the arithmetic average of the curves calculated for n and n – 1,[22] that is, in our case, $\chi_{17+18} \equiv (\chi_{17}+\chi_{18})/2$ (we will refer to this curve as n = 17+18). The susceptibility curves corresponding to the formulas of Baker et al. and Estes et al. and to the finite-size calculations for n = 17, 18, and 17+18 are compared to the (quasi-)exact result of Johnston et al. in Figure 6 in order to establish their ranges of validity.

All of the curves shown reproduce the characteristic maximum at $kT/|2J|$ = 0.6409; the curve of Baker et al., however, does so only nearly. At lower temperatures, this curve drops off very quickly, and hence the formula of Baker et al. applies to temperatures above that of the characteristic maximum. The curve of Estes et al. captures the maximum very well, and also reproduces the zero-temperature value almost exactly (it is too low by 2%). In the temperature range below $kT/|2J| < 0.25$, however, the predicted susceptibility is significantly too low, and hence the formula of Estes et al. works well for temperatures above $kT/|2J| > 0.25$. The finite-size calculations also reproduce the maximum very well, but show the expected deviations at low temperatures. The ground state of an antiferromagnetic chain with an even number of sites is a singlet, such that the magnetic susceptibility approaches zero for $T \rightarrow 0$. For a chain with odd n, the ground state is a doublet of two S = 1/2 multiplets, and the magnetic susceptibility shows Curie behaviour at low temperatures, that is it tends to infinity as T goes to zero.[22] The temperature at which the finite-size curves deviate from the exact curve decreases with increasing chain length, n. For the n = 17 and n = 18 curves, deviations become significant for $kT/|2J| < 0.25$. The curve for n = 17+18 shows a better performance, as expected,[22] and reproduces the exact magnetic susceptibility well for $kT/|2J| > 0.2$. Recently, Feyerherm et al.[26] provided the approximation [Equation (2)]

$$\chi(t) = \frac{N_A g^2 \mu_B{}^2}{4|2J|t} \frac{1 + 0.08516t^{-1} + 0.23351t^{-2}}{1 + 0.73382t^{-1} + 0.13696t^{-2} + 0.53568t^{-3}} \quad (2)$$

where $t = kT/|2J|$, which approximates the exact magnetic susceptibility very well for $kT/|2J| > 0.05$. This equation is probably the most useful one from a practical point of view (it is much simpler than the formula of Johnston et al., but at the cost of not being valid at the lowest temperatures).

The formula of Johnston et al. permitted a fit of the magnetic susceptibility data for **1**, which yielded the parameters $2J$ = –0.61(1) cm^{-1} and g = 2.11(1). The resulting curve is presented in Figure 4 and demonstrates excellent agreement with the data. As inferred already in the above discussion

of the magnetic data, the exchange interaction is antiferromagnetic and rather weak. It is noteworthy that so far the analysis of the $\chi_M T$ curve could have been attained with any of the methods/formulas described above, since $kT/|2J| > 2$ for the present experiment, a temperature range in which all discussed methods work very well.

An unambiguous confirmation of the exchange interactions in **1** comes from an analysis of the magnetization curve at 1.9 K. To the best of our knowledge, no formula suitable for an analysis of $M(B)$ data has been given so far (however, for $T = 0$ the magnetization curve is known exactly[16]). The finite-size calculations, however, in the course of which the full energy spectrum (at zero magnetic field) of a finite chain is obtained, also permit the calculation of the magnetic moment for arbitrary temperature and magnetic field via [Equation (3)][24–25]

$$M(T,B) = N_A \mu_B g \frac{\sum_{S\alpha} S B_S(gSx) \sinh[g(S+½)x] \exp[-E_{S\alpha}/(k_B T)]}{\sum_{S\alpha} \sinh[g(S+½)x] \exp[-E_{S\alpha}/(k_B T)]} \quad (3)$$

where $B_S(y)$ is the Brillouin function, $x = \mu_B B/(k_B T)$, and $E_{S\alpha}$ denotes the energy levels at zero magnetic field. It is easy to confirm that, for $B \rightarrow 0$, Equation (3) reduces to the Van Vleck equation for the susceptibility.[21] By using Equation (3), the magnetization curves of $n = 17$ and $n = 18$ chains at 1.9 K were calculated for the best-fit parameters deduced from the magnetic susceptibility. The curves for $n = 17$ and $n = 18$ are indistinguishable, as expected in view of the findings for the magnetic susceptibility (see Figure 6). The calculated $M(B)$ curve is presented in Figure 5, and it reproduces the experimental data very well. The theoretical curve is slightly too low at the highest field. This could be improved by the use of a slightly larger g value of 2.12, which is still, however, within the experimental error.

It is interesting to discuss the orientation of the magnetic orbitals of the Cu^{II} ions and the exchange pathway in some more detail. The Cu^{II} ions in **1** are in an elongated octahedral environment. The two nitrogen atoms of the bridging bipyridine ligands and the two oxygen atoms of the nitrophthalic ligands, with bond lengths of 1.967(2) Å for Cu(1)–O(1A) and Cu(1)–O(1B), 2.018(2) Å for Cu(1)–N(2), and 2.015(2) Å for Cu(1)–N(3), form the equatorial plane of the bipyramid, and the other two oxygen atoms of the nitrophthalic ligands, with bond lengths of 2.597(2) Å for Cu(1)–O(2A) and Cu(1)–O(2B), fill the axial positions. In this 4 + 2 coordination mode, the magnetic orbital is of the $d_{x^2-y^2}$ type, with the four lobes pointing towards the bipyridine nitrogen and nitrophthalic oxygen atoms. The Cu–N bond relevant for the exchange interaction is hence predominantly of σ-type. The magnetic orbitals on two neighboring Cu^{II} ions point almost directly towards each other, a situation which should be ideal for promoting antiferromagnetic interactions because it maximizes the orbital overlap. However, because of the σ-bonding, the magnetic orbitals on the Cu^{II} ions do not interact with the π-system of the bipyridine bridges, which could transmit exchange interactions efficiently, and hence a weak exchange interaction occurs.

The absence of any exchange interaction in the 4,4′-bipyridine-bridged chain, $[Cu(4,4'\text{-bpy})_3(DMSO)_2](ClO_4)_2 \cdot 2(4,4'\text{-bpy})$ (**2**), was explained by the twist of the two pyridyl rings of the bipyridine bridge by an angle of 61.4°.[1] In **1**, there is also such a twist, but with a smaller angle of 28.1(2)°. Therefore, it might be tempting to attribute the different exchange coupling strengths in **1** and **2** to this twist angle. However, considering the rotation-symmetric σ-character of the exchange pathway in **1** and **2**, a dependence on the twist angle should not exist.

Aside from **2**, few other one-dimensional chains containing 4,4′-bpy-bridged Cu^{II} ions have been analyzed (Table 4).[10b,27–28] Julve et al.[27] predicted a maximum coupling of $2J = -0.9$ cm^{-1} for these systems by using extended Hückel calculations, and the coupling in **1** lies comfortably within this limit. The larger couplings reported in ref.[10b] imply that the interaction modelled there may be of an intermolecular nature rather than through the 4,4′-bpy bridge or that the Fisher $S = 1/2$ model used may not be appropriate given that this is a classical model and does not describe the quantum nature of the $S = 1/2$ spin chain accurately.

Conclusions

Compound **1** is a one-dimensional coordination polymer that is the first to include both 4,4′-bpy and monodeprotonated 3-nitrophthalic acid. The magnetic properties of **1** are consistent with its structure and have been reproduced well in both magnetic susceptibility and magnetization curves. The comparison of several methods for calculating the magnetic susceptibility of one-dimensional antiferromagnetic $S = 1/2$ chains shows that for $kT/|2J| > 0.75$, all models, including finite-size calculations based on exact numerical diagonalization, are valid. This enabled us to also simulate the magnetization of **1** at 1.9 K, which confirmed the accuracy of our magnetic modelling. The weak antiferromagnetic coupling in **1** is within predicted ranges and is consistent with that of other similar materials.

Table 4. Values of $2J$ [cm^{-1}], g, and torsion angle [°] for the reported 4,4′-bpy-bridged Cu chains.

Compound	$2J$	g	Torsion angle	Ref.
$\{[Cu(\text{L-threoninato})(4,4'\text{-bpy})(H_2O)][NO_3]\}_n$	–1.01	2.016	17.1	[10b]
$\{[Cu(\text{L-alaninato})_2(4,4'\text{-bpy})(H_2O)_2]_2[NO_3]_4\}_n \cdot 6nH_2O$	–1.35	1.996	17.3	[10b]
$[Cu(NO_3)_2(2,2'\text{-bipy})(4,4'\text{-bpy})]_n \cdot 2nCH_3OH$	–0.53	2.01	0.0	[28]
$[Cu(4,4'\text{-bpy})_3(DMSO)_2](ClO_4)_2 \cdot 2(4,4'\text{-bpy})$	≈ 0	2.06	61.4	[1]
1	–0.61(1)	2.11(1)	28.1(2)	this work

Experimental Section

General: 3-Nitrophthalic acid, copper perchlorate and 4,4′-bipyridine were obtained from commercial sources and used without further purification. The IR spectra were recorded in the 4000–400 cm^{-1} range with a Bruker Equinox 55 FT-IR spectrometer using KBr pellets. Elemental analyses were performed with an Elemental Vario EL-3 elemental analyzer.

Synthesis of $[Cu^{II}(HL)_2(4,4'\text{-bpy})]_n \cdot 2nH_2O$ (1): An ethanol solution of 4,4′-bpy (0.16 g, 1.0 mmol) was added slowly to an aqueous solution of 3-nitrophthalic acid (0.42 g, 2.0 mmol) and $Cu(ClO_4)_2$ (0.37 g, 1.0 mmol). The resulting blue solution was allowed to stand at room temperature for 2 days to yield dark blue, block-shaped crystals (0.44 g, 65%). $C_{26}H_{20}CuN_4O_{14}$ (676.00): calcd. C 46.19, H 2.98, N 8.29; found C 46.13, H 3.03, N 8.32. IR: $\tilde{\nu}$ = 3360, 3170, 3015, 2939, 1695, 1615, 1454, 1406, 1328, 1273, 1186, 1149, 1115, 1049, 987, 813, 705, 653, 579, 505 cm^{-1}.

X-ray Crystallography: A single crystal of the title compound, **1**, with dimensions of $0.45 \times 0.42 \times 0.30$ mm^3 was measured with a Bruker Smart Apex II CCD diffractometer equipped with Mo-K_α radiation (λ = 0.71073 Å) at 293 K by using the ω scan mode. The data were corrected for empirical absorption with SADABS.[29] The structure was solved by direct methods and refined by full-matrix least-squares techniques with the SHELXL program.[30] The hydrogen atoms bonded to carbon and oxygen atoms (COOH) were included in idealized geometric positions with thermal parameters 1.2 (for C) or 1.5 (for O) times larger than those of the atoms to which they are attached. The hydrogen atoms of water molecules were located from the difference Fourier map with O–H 0.85(1) Å and U(H) = 0.08 $Å^2$ and were refined isotropically. Anisotropic displacement parameters were refined for all non-hydrogen atoms.

CCDC-663915 contains the supplementary crystallographic data for **1**. These data can be obtained free of charge from The Cambridge Crystallographic Data Centre via www.ccdc.cam.ac.uk/data_request/cif.

Magnetic Measurements: Variable-temperature magnetic susceptibility data (1.9–300 K, 0.1 T) and magnetization data (1.9 K, 0–5 T) were obtained using a Quantum Design MPMSXL SQUID magnetometer. The polycrystalline sample was prepared in a saran foil bag and placed inside a plastic straw for attachment to the sample transport rod. Background corrections for the sample holder and diamagnetic components of the compounds were made using Pascal's constants.

Supporting Information (see also the footnote on the first page of this article): The table of the constants used for the formula proposed by Johnston et al. and the formulas used to calculate the magnetic susceptibility.

Acknowledgments

This work was supported by the Beijing Talent Fund for Young Sci-Tech Researchers (grant no. H013610050112). Partial financial support from the EC-RTN-QUEMOLNA, contract no. MRTN-CT-2003-504880, and the Swiss National Science Foundation (grant no. 200020-116003) as well as from the European project "MAGMANet" is gratefully acknowledged.

[1] J. D. Woodward, R. Backov, K. A. Abboud, H. Ohnuki, M. W. Meisel, D. R. Talham, *Polyhedron* **2003**, *22*, 2821–2830.
[2] J. Jin, S. Y. Niu, G. D. Yang, L. Ye, *Z. Anorg. Allg. Chem.* **2006**, *632*, 2350–2354.
[3] D. Hagrman, C. Zubieta, D. J. Rose, J. Zubieta, R. C. Haushalter, *Angew. Chem. Int. Ed. Engl.* **1997**, *36*, 873–876.
[4] T. Korzeniak, K. Stadnicka, M. Rams, B. Sieklucka, *Inorg. Chem.* **2004**, *43*, 4811–4813.
[5] E. Barea, M. Quiros, J. A. R. Navarro, J. M. Salas, *Dalton Trans.* **2005**, 1743–1746.
[6] S. Noro, R. Kitaura, M. Kondo, S. Kitagawa, T. Ishii, H. Matsuzaka, M. Yamashita, *J. Am. Chem. Soc.* **2002**, *124*, 2568–2583.
[7] C. Inman, J. M. Knaust, S. W. Keller, *Chem. Commun.* **2002**, 156–157.
[8] B. P. Yang, J. G. Mao, *Inorg. Chem.* **2005**, *44*, 566–571.
[9] a) D. Braga, A. Angeloni, L. Maini, A. W. Götz, F. Grepioni, *New J. Chem.* **1999**, *23*, 17–24; b) C. Bielawski, Y.-S. Chen, P. Zhang, P.-J. Prest, J. S. Moore, *Chem. Commun.* **1998**, 1313–1314; c) A. D. Burrows, S. Menzer, D. M. P. Mingos, A. J. P. White, D. J. Williams, *J. Chem. Soc. Dalton Trans.* **1997**, 4237–4240; d) C. Janiak, *Dalton Trans.* **2003**, 2781–2804; e) S. G. Baca, I. G. Filippova, C. Ambrus, M. Gdaniec, Y. A. Simonov, N. Gerbeleu, O. A. Gherco, S. Decurtins, *Eur. J. Inorg. Chem.* **2005**, 3118–3130; f) S. G. Baca, I. G. Filippova, O. A. Gherco, M. Gdaniec, Y. A. Simonov, N. V. Gerbeleu, P. Franz, R. Basler, S. Decurtins, *Inorg. Chim. Acta* **2004**, *357*, 3419–3429.
[10] a) L. G. Zhu, S. Kitagawa, H. Miyasaka, H. C. Chang, *Inorg. Chim. Acta* **2003**, *355*, 121–126; b) B. Y. Lou, R. H. Wang, D. Q. Yuan, B. L. Wu, F. L. Jiang, M. C. Hong, *Inorg. Chem. Commun.* **2005**, *8*, 971–974; c) B. Y. Lou, F. L. Jiang, B. L. Wu, D. Q. Yuan, M. C. Hong, *Cryst. Growth Des.* **2006**, *6*, 989–993.
[11] a) M.-L. Tong, H.-J. Chen, X.-M. Chen, *Inorg. Chem.* **2000**, *39*, 2235–2238; b) R.-H. Wang, F.-L. Jiang, Y.-F. Zhou, L. Han, M.-C. Hong, *Inorg. Chim. Acta* **2005**, *358*, 545–554; c) J.-L. Lin, Y.-Q. Zheng, *Acta Crystallogr., Sect. C* **2005**, *61*, m501–m503; d) J. Tao, X. Yin, R.-B. Huang, L.-S. Zheng, *Inorg. Chem. Commun.* **2002**, *5*, 1000–1002.
[12] a) Y.-H. Wen, J.-K. Cheng, Y.-L. Feng, J. Zhang, Z.-J. Li, Y.-G. Yao, *Inorg. Chim. Acta* **2005**, *358*, 3347–3354; b) S. Dalai, P. Mukherjee, E. Zangrando, F. Lloret, N. Chaudhuri, *J. Chem. Soc. Dalton Trans.* **2002**, 822–823; c) X.-Q. Lu, J.-J. Jiang, C.-L. Chen, B.-S. Kang, C.-Y. Su, *Inorg. Chem.* **2005**, *44*, 4515–4521; d) R.-F. Hu, Y. Kang, J. Zhang, Z.-J. Li, Y.-Y. Qin, Y.-G. Yao, *Z. Anorg. Allg. Chem.* **2005**, *631*, 3053–3057; e) B. Rather, M. J. Zaworotko, *Chem. Commun.* **2003**, 830–831; f) C.-Y. Sun, L.-P. Jin, *J. Mol. Struct.* **2006**, *782*, 171–176; g) D.-Y. Kong, J. Zon, J. McBee, A. Clearfield, *Inorg. Chem.* **2006**, *45*, 977–986.
[13] X.-Q. Shen, H.-B. Qiao, Z.-J. Li, H.-Y. Zhang, H.-L. Liu, R. Yang, P.-K. Chen, H.-W. Hou, *Inorg. Chim. Acta* **2006**, *359*, 642–648.
[14] Y.-H. Deng, S.-Y. Wang, J. Liu, Y.-L. Yang, F. Zhang, H.-W. Ma, *Acta Chim. Sinica* **2007**, *65*, 809–815.
[15] Y.-H. Deng, J. Liu, Y.-L. Yang, H.-J. Zhu, H.-W. Ma, *Chin. J. Struct. Chem.* **2007**, *26*, 642–648.
[16] S. Eggert, I. Affleck, M. Takahashi, *Phys. Rev. Lett.* **1994**, *73*, 332–335.
[17] D. C. Johnston, R. K. Kremer, M. Troyer, W. Wang, A. Klümper, S. L. Bud'ko, A. F. Panchula, P. C. Canfield, *Phys. Rev. B* **2000**, *61*, 9558–9606.
[18] R. B. Griffiths, *Phys. Rev.* **1964**, *133*, A768–A775.
[19] G. A. Baker, G. S. Rushbrooke, H. E. Gilbert, *Phys. Rev.* **1964**, *135*, A1272–A1277.
[20] W. E. Estes, D. P. Gavel, W. E. Hatfield, D. Hodgson, *Inorg. Chem.* **1978**, *17*, 1415–1421.
[21] O. Kahn, *Molecular Magnetism*, VCH Publishers, New York, **1993**.

[22] J. C. Bonner, M. E. Fisher, *Phys. Rev. A* **1964**, *135*, 640–658.
[23] D. Gatteschi, L. Pardi, *Gazz. Chim. Ital.* **1993**, *123*, 231–240.
[24] O. Waldmann, *Phys. Rev. B* **2000**, *61*, 6138–6144.
[25] O. Waldmann, H. U. Güdel, T. L. Kelly, L. K. Thompson, *Inorg. Chem.* **2006**, *45*, 3295–3300.
[26] R. Feyerherm, S. Abens, D. Günther, T. Ishida, M. Meissner, M. Meschke, T. Nogami, M. Steiner, *J. Phys.: Condens. Matter* **2000**, *12*, 8495–8509.
[27] M. Julve, M. Verdaguer, J. Faus, F. Tinti, J. Moratal, Á. Monge, E. Gutiérrez-Puebla, *Inorg. Chem.* **1987**, *26*, 3520–3527.
[28] H. W. Park, S. M. Sung, K. S. Min, H. Bang, M. P. Suh, *Eur. J. Inorg. Chem.* **2001**, 2857–2863.
[29] G. M. Sheldrick, *SADABS. Program for Empirical Absorption Correction of Area Detector Data*, University of Göttingen, Germany, **1996**.
[30] G. M. Sheldrick, *SHELXTL*, version 6.10, Bruker Analytical X-ray Systems, Madison, WI, **2001**.

Received: October 18, 2007
Published Online: February 12, 2008

